Study of Electron Transport in SOI MOSFETs using Monte Carlo Techinique with Full-Band Modeling

H. Takeda, N. Mori and C. Hamaguchi

Department of Electronic Engineering, Osaka University
2–1 Yamada-oka, Suita City, Osaka 565-0871, Japan
takeda@ele.eng.osaka-u.ac.jp

Abstract

In SOI MOSFETs, electrons are quantized into two-dimensional electron gas by the strong electric field normal to the interface. When the Si-layer thickness is thinner than the inversion layer width, the confinement becomes stronger and effects of the non-parabolicity of the Si band structure will significantly influence the two-dimensional electronic states. We studied effects of the non-parabolicity on the electronic states in SOI MOSFETs with such an ultra-thin Si-layer by using an empirical pseudo-potential method and analyzed the electron transport properties by performing single-electron Monte Carlo simulations.

Keywords: SOI MOSFET, pseudo-potential method, Monte Carlo simulation, non-parabolicity

1 Introduction

Electrons in SOI MOSFETs are quantized into two-dimensional electron gas (2DEG) by the gate electric field applied perpendicular to the Si/SiO_2 interface. The transport properties are considered to be strongly affected by this quantization. Especially, in SOI MOSFETs with an ultra thin Si-layer, such quantization effects become stronger and the effects on the electron transport properties can be more significant. When electrons are quantized along the (001)-direction, the ellipsoidal 6-fold valleys of the Si conduction band split into 2-fold and 4-fold valleys. The 2-fold and 4-fold valleys are quantized along the longitudinal and the transverse axes, respectively. It has been reported that the strong confinement causes large energy splits between subbands of the two ladders and electrons accumulate mainly in the 2-fold valleys, whose effective mass parallel to the interface is lighter than that in the 4-fold valleys, resulting in an electron mobility enhancement [1]. For such a thin Si-film, the non-parabolicity of the conduction band structure will significantly affect the electron transport properties because of increase in the electron occupation of the 2-fold valleys. We have been investigating the effects of the non-parabolicity by using an empirical pseudo-potential method [2], [3]. In the present work, we have studied the electronic states by self-consistently solving the Schrödinger and Poisson equations based on a new scheme. We have then carried out single-electron Monte Carlo simulations by using the self-consistently obtained electronics states.

2 Pseudo-Potential Method

The Schrödinger equation for a bulk-crystal with no external potential is expressed as following

$$\left\{-\frac{\hbar^2}{2m}\nabla^2 + V_{\rm P}(\mathbf{R})\right\}\psi(\mathbf{R}) = \mathcal{E}\psi(\mathbf{R}), \tag{1}$$

where $V_{\rm P}$ is a pseudo-potential. Expanding the wave function ψ by Bloch functions $u^n_{\mathbf{K}} = \sum_{\mathbf{G}} f^n_{\mathbf{K}}(\mathbf{G})\mathrm{e}^{i\mathbf{G}\cdot\mathbf{R}}$ as

$$\psi^n_{\mathbf{K}}(\mathbf{R}) = \mathrm{e}^{i\mathbf{K}\cdot\mathbf{R}}u^n_{\mathbf{K}} = \mathrm{e}^{i\mathbf{K}\cdot\mathbf{R}}\sum_{\mathbf{G}} f^n_{\mathbf{K}}(\mathbf{G})\,\mathrm{e}^{i\mathbf{G}\cdot\mathbf{R}}, \tag{2}$$

we have

$$\frac{\hbar^2}{2m}(\mathbf{K}+\mathbf{G})^2 f^n_{\mathbf{K}}(\mathbf{G}) + \sum_{\mathbf{G}'} V_{\rm P}(\mathbf{G}-\mathbf{G}')f^n_{\mathbf{K}}(\mathbf{G}') = \mathcal{E}^n(\mathbf{K})f^n_{\mathbf{K}}(\mathbf{G}), \tag{3}$$

where n is the band index, and $\mathbf{K}$ and $\mathbf{G}$ represent three-dimensional wave vector and reciprocal lattice vector, respectively [4].

In a Si-layer of SOI MOSFETs, we have an additional external one-dimensional confining potential $U(z)$, and the Schrödinger equation is written as

$$\left\{-\frac{\hbar^2}{2m}\nabla^2 + V_{\rm P}(\mathbf{R}) + U(z)\right\}\Psi(\mathbf{R}) = E\Psi(\mathbf{R}). \tag{4}$$

By expanding the wave functions Ψ for 2DEG with bulk wave functions $\psi^n_{\mathbf{K}}$ as $\Psi = \sum_{\mathbf{K},n} c^n_{\mathbf{K}}\psi^n_{\mathbf{K}}$, equation (4) becomes

$$\sum_{k'_z,n'}\left[\mathcal{E}^{n'}(\mathbf{k},k'_z)\delta_{n,n'}\delta_{k'_z,k_z} + \sum_{\mathbf{G},g'_z} f^{n*}_{\mathbf{k},k_z}(\mathbf{G})f^{n'}_{\mathbf{k},k'_z}(\mathbf{g},g'_z) \times U_{\rm F}(k'_z - k_z + g'_z - g_z)\right]c^{n'}_{\mathbf{k},k'_z} = E(\mathbf{k})\,c^n_{\mathbf{k},k_z}, \tag{5}$$

where

$$U_{\rm F}(q_z) = \frac{1}{L}\int_0^L U(z)\mathrm{e}^{iq_z z}dz \tag{6}$$

with L being the length of the system. In the previous study [2], [3], we assumed that $U(z)$ is slowly varying and $U_{\rm F}(q_z)$ can be approximated as $U_{\rm F}(k_z - k'_z + g_z - g'_z)|_{g'_z \neq g_z} = 0$. In the present work, we fully take into account g_z-dependence of $U_{\rm F}(q_z)$. Figure 1 shows the potential profiles for $L_{\rm Si} = 5.43\,{\rm nm}$ obtained by performing an inverse Fourier transform of $U_{\rm F}(q_z)$ neglecting the g_z-dependence (dashed line) and including the g_z-dependence (lighter solid line) together with the original $U(z)$ profile (dark solid line). We see that g_z-dependence should be taken into account for accurately expressing $U(z)$ in the case of thin Si-film.

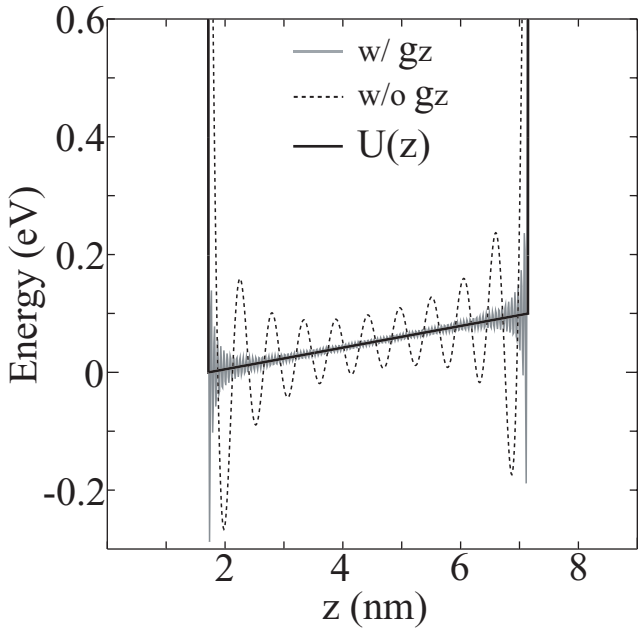

Figure 1: Potential profiles obtained by performing an inverse Fourier transform of $U_{\rm F}(q_z)$ neglecting the g_z-dependence (dashed line) and including the g_z-dependence (lighter solid line) together with the original $U(z)$ profile (dark solid line) for $L_{\rm Si} = 5.43\,{\rm nm}$.

We have solved the Schrödinger equation of Eq. (5) combining Poisson equation within a Hartree approximation. In such a self-consistent calculation, we need to evaluate electron charge distribution along z. For evaluating the electron charge distribution, we calculated the density of states of 2DEG by the following method. The two-dimensional **k**-space is discretized into rectangle meshes and the density of states of each mesh are assumed to be equally distributed between the maximum and minimum energy of the corner-point energies calculated from Eq. (5). Although the boundary of 2-fold and 4-fold valleys is not clearly defined, we arbitrarily define the boundary in the following calculation [5].

For studying effects of the non-parabolicity of the conduction band structure on electronic states, we also calculated the electron states using a simple parabolic band structure based on an effective mass approximation. We call the calculation model using the pseudo-potential method described above as "pseudo-potential model", and that using the effective mass approximation as "parabolic model".

In Fig. 2 we plot squared wave functions at the bottom of each valley and potential profile self-consistently evaluated with the pseudo-potential model (solid lines) and with the parabolic model (dashed lines). The calculation conditions are as follows; the thickness of Si-layer is $L_{\rm Si} = 5.43\,{\rm nm}$, the lattice temperature is $T = 300\,{\rm K}$, the electron sheet density is $N_{\rm s} = 4.0 \times 10^{12}\,{\rm cm}^{-2}$, and the voltage difference along z is $\Delta V_{\rm Si} = 0.1\,{\rm V}$. In the parabolic model, we use the same $U(z)$ as that obtained with the pseudo-potential model, and the effective masses along the transverse and longitudinal axis are set to be $0.199m_0$ and $0.877m_0$, respectively, which are calculated from the energy dispersions of the bulk conduction band with the empirical pseudo-potential method [6]. The subband energies are not so much different between the two models. Especially, the difference is vanishingly small for the 2-fold valleys. Note that the wave functions for the pseudo-potential model oscillate because they include the Bloch terms.

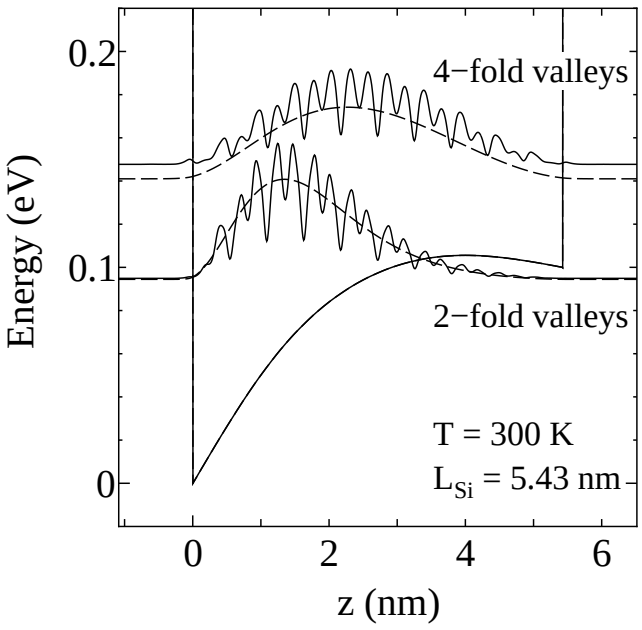

Figure 2: Potential profile and the squared wave functions at the bottom of the 2-fold and the 4-fold valleys calculated with the pseudo-potential (solid lines) and the parabolic (dashed lines) models.

3 Scattering Rate

To perform a Monte Carlo simulation, we calculated electron scattering rates using the electronic states obtained by the self-consistent method with the full-band modeling. In the present study, we consider intra-valley scattering via acoustic phonons and inter-valley scattering via acoustic or optic phonons as scattering processes, because those scattering mechanisms are intrinsic and dominant at the room temperature.

The intra-valley phonon scattering rate $1/\tau^{\mu}_{\rm intra}(\mathbf{k})$ which an electron at $\mathbf{k} = (k_x, k_y)$ in subband μ is scattered into $\mathbf{k}' = (k'_x, k'_y)$ in subband ν is calculated by the following equation:

$$\frac{1}{\tau^{\mu}_{\rm intra}(\mathbf{k})} = \frac{k_B T}{\hbar \rho v_s^2} \sum_{\nu} \sum_{k'_x, k'_y} G^{\nu}_{k'_x, k'_y}(E^{\mu}(\mathbf{k})) \times \int \Delta^2(\mathbf{k}' - \mathbf{k}, q_z) |\mathcal{F}_{\mu,\nu}(q_z)|^2 dq_z, \quad (7)$$

where $\mathbf{Q} = (q_x, q_y, q_z)$ represents a phonon wave vector, ρ is the density of Si, v_s is the sound velocity, $E^{\mu}(\mathbf{k})$ is the energy eigenvalue obtained from Eq. (5) and $G^{\mu}_{k_x,k_y}(E^{\mu}(\mathbf{k}))$ is the state density. Equation (7) includes both phonon emission and absorption processes within an equi-partition approximation. We consider longitudinal acoustic (LA) and transverse acoustic (TA) phonons. The deformation potential, $\Delta(\mathbf{k})$, for each phonon mode is given by

$$\Delta_{\rm LA}(\theta_Q) = \Xi_d + \Xi_u \cos^2(\theta_Q), \quad (8)$$

$$\Delta_{\rm TA}(\theta_Q) = \Xi_u \cos^2(\theta_Q) \sin(\theta_Q). \quad (9)$$

In Eq. (8), $\Xi_u = 9.0\,{\rm eV}$, $\Xi_d = -11.7\,{\rm eV}$ and θ_Q is the angle between phonon wave vector $\mathbf{Q}$ and the longitudinal axis of each valley [4]. The form factor $\mathcal{F}_{\mu,\nu}(q_z)$ is defined by the following equation:

$$\mathcal{F}_{\mu,\nu}(q_z) = \int \Psi^{\nu *}_{\mathbf{k}_0}(z) {\rm e}^{iq_z \cdot z} \Psi^{\mu}_{\mathbf{k}_0}(z) dz. \quad (10)$$

The inter-valley phonon scattering rate $1/\tau^{\mu}_{\rm inter}(\mathbf{k})$ is calculated by the following equation

$$\frac{1}{\tau^{\mu}_{\rm inter}(\mathbf{k})} = \frac{\Delta^2}{2\rho\omega_Q} \sum_{\nu} \int dq_z |\mathcal{F}_{\mu,\nu}(q_z)|^2 \times \sum_{k'_x, k'_y} \Big[N_Q G^{\nu}_{k'_x, k'_y}(E^{\mu}(\mathbf{k}) + \hbar\omega_Q) + (N_Q + 1) G^{\nu}_{k'_x, k'_y}(E^{\mu}(\mathbf{k}) - \hbar\omega_Q) \Big], \quad (11)$$

where $N_Q = 1/\{\exp(\hbar\omega_Q/k_{\rm B}T) - 1\}$. We take account of g-processes via TA, LA, and longitudinal optic (LO) phonons, and f-processes via TA, LA, and transverse optic (TO) phonons as inter-valley scattering processes. We use the values of the deformation potential and the phonon energy for each scattering process as in Ref. [4].

Figure 3 shows the total scattering rate of the lowest subband in the 2-fold valleys as a function of the electron energy. The closed circles and the solid line represent the calculated results of the pseudo-potential model and the parabolic model, respectively.

For the electron energy lower than about 0.15 eV, we hardly see a difference between the two models. When the electron energy is higher than about 0.15 eV, the scattering rate of the pseudo-potential model becomes larger than that of the parabolic model because of larger density of states for the pseudo-potential model.

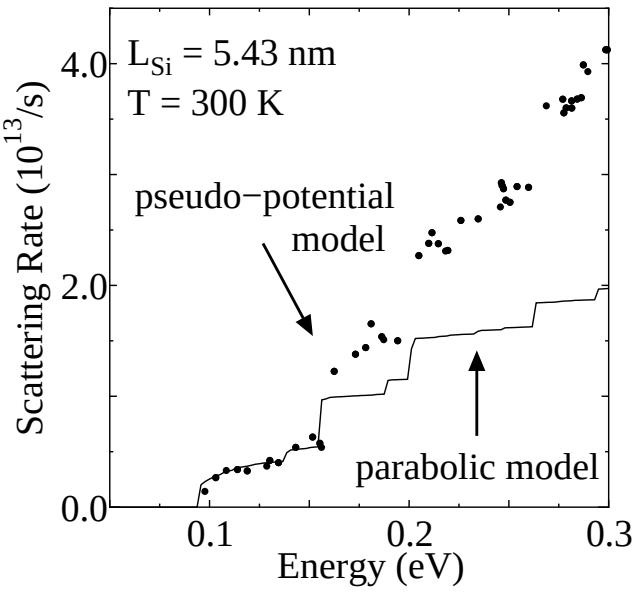

Figure 3: Total scattering rates of the lowest subband in the 2-fold valleys calculated with the pseudo-potential (closed circles) and the parabolic (solid lines) models.

4 Monte Carlo Simulation

We carried out single-electron Monte Carlo simulations using the scattering rates obtained above. In the pseudo-potential model, the scattering rates are assumed to be constant within a discretized $\mathbf{k}$-mesh. Figure 4 shows the electron drift-velocity versus the parallel electric field. The drift-velocity of the pseudo-potential model is plotted by the closed circles and those of the parabolic model are plotted by the open circles. The electric field parallel to the Si/SiO_2 interface is applied along (100)-direction. We see that the drift-velocity is strongly affected by the non-parabolicity of subband structures. The difference in drift-velocities increases as

the electric field increase. This is because that average electron energy increases under higher applied electric fields and electrons with higher kinetic energy are strongly affected by the non-parabolicity.

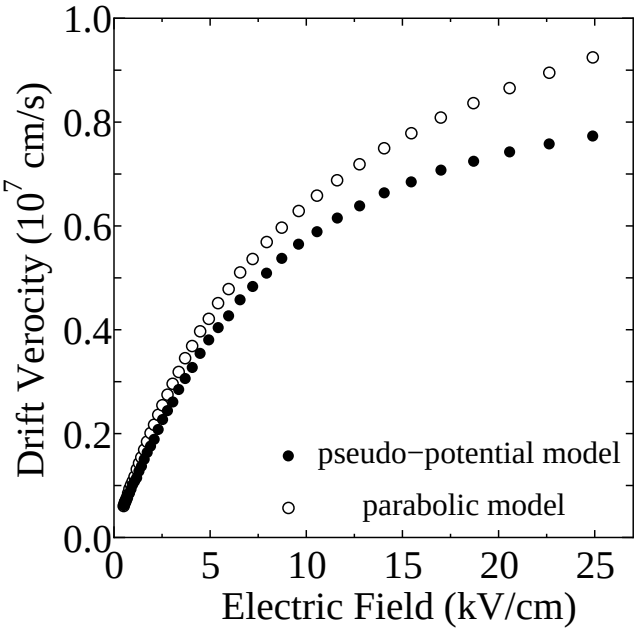

Figure 4: Drift-velocities versus applied parallel electric field obtained by the Monte Carlo simulation. Closed and open circles are the drift-velocities of the pseudo-potential model and the parabolic model, respectively.

5 Summary

In order to study effects of the non-parabolicity of the subband structure on the two-dimensional electronic states in SOI MOSFETs, we solved the Schrödinger and Poisson equations self-consistently using the empirical pseudo-potential method and Hartree approximation. Using the electronic states evaluated from the self-consistent method, we calculated the phonon scattering rates. We then carried out the Monte Carlo simulations with the scattering rates that included the effects of non-parabolicity of the energy band structure. We find that the non-parabolicity of the conduction band structure strongly influences the electron drift-velocity.

REFERENCES

[1] S. Takagi, J. Koga and A. Toriumi, Jpn. J. Appl. Phys. **37**, 1289 (1998).

[2] H. Takeda, N. Mori, and C. Hamaguchi, presented at 12th International Conference on Nonequilibrium Carrier Dynamics in Semiconductors, La Fonda Hotel, Santa Fe, New Mexico, USA, August 27-31, 2001.

[3] H. Takeda, N. Mori, and C. Hamaguchi, presented at the 8th International Workshop on Computational Electronics, Beckman Institute, University of Illinois, USA, October 15-18, 2001.

[4] M.V. Fischetti and S.E. Laux, Phys. Rev. B **48**, 2244 (1993).

[5] M.V. Fischetti and S.E. Laux, Phys. Rev. B **38** 9721 (1988).

[6] J. Chelikowsky, D.J. Chadi, and Marvin L. Cohen, Phys. Rev. B **8**, 2786 (1973).